Engineering Geology 115 (2010) 209–216

Contents lists available at ScienceDirect

Engineering Geology

journal homepage: www.elsevier.com/locate/enggeo

Anisotropic behaviour of White Macael marble used in the Alhambra of Granada (Spain)
The role of thermohydric expansion in stone durability

A. Luque [a,*], G. Cultrone [a], S. Mosch [b], S. Siegesmund [b], E. Sebastian [a], B. Leiss [c]

[a] Departamento de Mineralogía y Petrología, Universidad de Granada, Avenida Fuentenueva s/n, 18002, Granada, Spain
[b] Geowissenschaftliches Zentrum der Universität Göttingen, Golschmidstrße 3, 37077 Göttiengen, Germany
[c] Institute of Geology Dynamics of the Lithosphere (IGDL), Universität Göttingen, Golschmidstrße 3, 37077 Göttiengen, Germany

ARTICLE INFO

Article history:
Received 17 February 2009
Received in revised form 25 May 2009
Accepted 25 June 2009
Available online 6 July 2009

Keywords:
White Macael marble
Durability
Thermal expansion
Microfabric
Residual strain

ABSTRACT

One of the most commonly used marbles in Spain is "White Macael" marble, quarried in the Macael area of Almeria. Throughout Spanish history, White Macael has been in great demand as an ornamental stone and was used to build pieces of great importance and artistic beauty, such as the Fountain of Lions in the Alhambra (Granada).
Over the centuries, such pieces have suffered from decay due to exposure to the elements, as has happened in many other marbles all over the world.
The main purpose of this paper was to determine the durability of White Macael marble when subjected to changes in thermal conditions. It was observed that these changes in the presence of humidity were an important factor in marble decay. They produce a progressive loss of cohesion along grain boundaries and an increase in porosity, which are starting points for marble degradation and facilitate the development of other pathologies.

1. Introduction

Marble has been popular as a construction and ornamental stone throughout history because of its aesthetic and physical properties (i.e. hardness, very low porosity, etc.).

In recent decades marble used in building façades has suffered serious deterioration problems (bowing, granular disintegration, flaking and cracks), in some cases after only relatively few years exposure.

Researchers investigating the deterioration observed in certain well-known modern buildings, focused on the durability of marble and showed that the alternation of heat and cold cycles under moisture conditions was the main factor influencing its decay (Malaga et al., 2008; Siegesmund et al., 2008; Koch and Siegesmund, 2004; Widhalm et al., 1996).

Early research into the physical and mechanical behaviour of marbles by Kessler (1919) determined that the processes of thermal expansion in marbles were responsible for their initial decay. More recently, Thomasen and Ewart (1984) and Bortz et al. (1988) investigated what variations in the moisture content during decay processes could be responsible for the ultimate decay of the marble. Bland and Rolls (1998) found that marble is very sensitive to temperature changes, which cause granular disintegration.

Siegesmund et al. (1999) proved that one of the main factors that influences marbles' physical, mechanical and hydric properties are fabric and textural anisotropy (i.e. grain size, shape and orientation). Preferred lattice orientation and grain fabric (morphology and geometry of grain boundary) play a basic role in marble deterioration (Siegesmund et al., 2000; Royer-Carfagni, 2000; Zeisig et al., 2002; Cantisani et al., 2009; Åkesson et al., 2006). In addition, the characterization of physical parameters such as thermal expansion, thermal conductivity and elastic wave velocity clearly demonstrates that fabric analysis can help to predict stone durability (Widhalm et al., 1997; Weiss et al., 2000; Sáez-Pérez and Rodríguez-Gordillo, 2009).

Weiss et al. (2002, 2003) demonstrated that anisotropic thermal expansion in marble produced a progressive loss of cohesion along the grain boundaries, which led to an initial state of decay. In addition, Koch and Siegesmund (2002, 2004) pointed out that the formation of bowing is directly controlled by cyclic variations of temperature in the presence of water.

An example of the anisotropic behaviour of marbles is the residual strain presented by these stones at the end of thermal expansion tests (Siegesmund et al., 1999, Leiss and Weiss, 2000). These tests have also demonstrated that continuous heat–cold cycles favour marble elongation which in many cases coincides with the *c*-axis orientation of calcite

* Corresponding author. Dep. Mineralogy and Petrology, Faculty of Science, University of Granada, Avenida Fuentenueva s/n, 18002, Granada, Spain.
E-mail address: analuque@ugr.es (A. Luque).

0013-7952/$ – see front matter © 2009 Elsevier B.V. All rights reserved.
doi:10.1016/j.enggeo.2009.06.015

crystals (Koch and Siegesmund, 2004; Siegesmund et al., 2000; Widhalm et al., 1996; Battaglia et al., 1993).

In this work we will be analyzing White Macael (WM), a marble that was widely used in Spain's Architectural Heritage and which remains today one of Spain's most commonly exported building stones. Of all the artworks sculpted with WM, the Fountain of the Lions in the Alhambra (Granada, Spain) is perhaps the most outstanding because of its exquisite decorations (Fig. 1).

This fountain is one of the best examples of 11th century Islamic art. Twelve lions stand in a circle supporting the basin of the fountain. The water flows out through the mouth of the lions and then along four channels that divide the courtyard into equal quadrants.

Bello et al. (1992) and Galán and Zezza, (1990) linked the state of decay of this fountain to the environmental conditions in the courtyard. Using ultrasound, Zezza and Sebastián Pardo (1992) discovered a marked anisotropy along WM foliation planes that were not easily distinguishable to the naked eye.

Rodríguez-Gordillo and Sáez-Pérez (2006) made an initial study of the anisotropic behaviour of WM by carrying out heat–cold cycles on freshly quarried marbles. They observed marble deterioration (i.e. loss of small fragments) caused by thermal expansion in wet conditions, but they did not quantify either the degree of anisotropy or the amount of deterioration. These authors found that microfabric, the existence of microcracks and the preferred orientation of crystallographic axes are the factors that most affect the behaviour of marble with respect to temperature changes. The geometric disposition of crystals in microfabric is of great importance, since the marbles with hexagonal-shaped crystals and straight joints are the least resistant to thermal changes. Furthermore, the existence of microcracks and their spatial disposition is the main way for other decay agents (e.g. soluble salts) to enter the stone. Microcracks will grow or expand inside the stone so producing an increase in fissure porosity. In calcitic marbles the main expansion factor is the preferred crystallographic orientation, as calcite is a strongly anisotropic mineral (Kleber, 1959). This means that the crystal expands along the *c*-axis and contracts along the *a*-axis of the mineral.

A detailed characterization of the anisotropic behaviour of WM during the thermohydric expansion test is one of the main goals of the present work, because of its relevance for conservation issues especially in fountains where cold and heat cycles can alternate frequently in the presence of water. In general, the characterization of the anisotropic thermal expansion that can take place in marbles is essential if we want to predict the future behaviour of this stone both in buildings and decorative pieces.

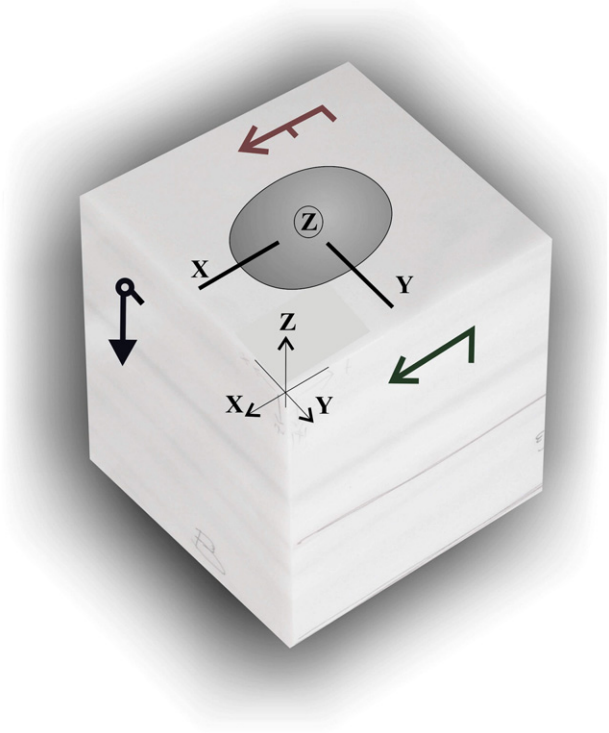

Fig. 2. Schematic representation of a marble cube with the disposition of reference axes according to the foliation planes. Schmidt pole figures are shown.

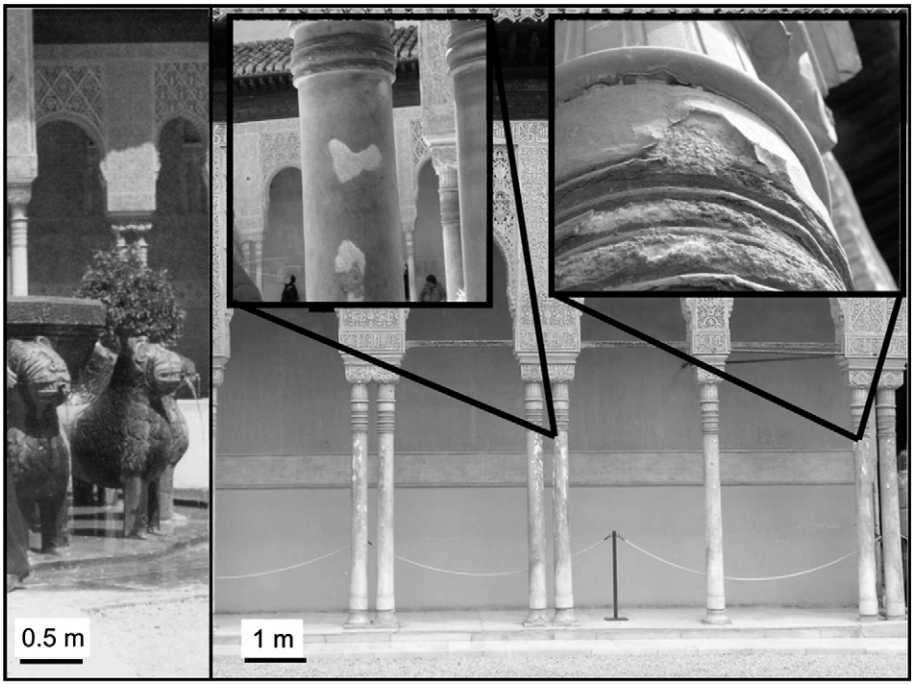

Fig. 1. General view and detailed images showing White Macael marble damage caused by granular disintegration and cracks, in most of the columns of the Courtyard of the Lions in the Alhambra of Granada (Spain).

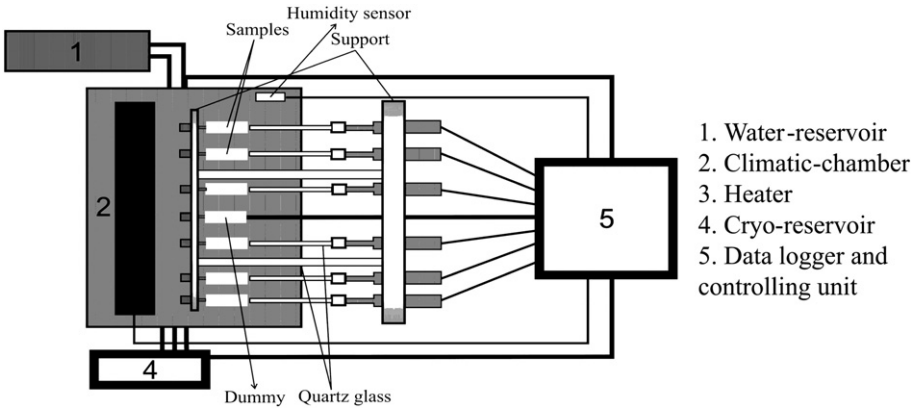

Fig. 3. Schematic representation of the orientation of the 6 cores tested with respect to the established coordinate system. Image of a pushrod dilatometer (Strohmeyer, 2004).

2. Materials and methods

2.1. Samples

As it is impossible to take samples from the Courtyard of Lions because of their historic value, we used freshly quarried blocks of White Macael marble (WM) from a quarry in the Macael area of Almeria (Spain), where the local economy largely depends on the quarrying of different types of marble.

WM is a pearly-white stone, but sometimes, depending on the particular quarrying area or strata, it may present a grey foliation which varies in the intensity of its colour and in the number of lines crossing the stone. This foliation is composed of muscovite, amphibole, epidote, titanite and deformed carbonate grains (López Sánchez-Vizcaíno et al., 1997).

From a geological point of view, WM is a Late Triassic marble that belongs to the Nevado-Filabride Complex in the so-called Betic Internal Zone, which is the lowest tectonic unit of the Alboran Domain (Balanyá and García-Dueñas, 1986).

The material selected for this research is characterized by some greyish layers which correspond to marble foliation planes. Block cubes of 50 cm edge were cut into different specimens. Prior to cutting, a reference-coordinate system was introduced to record the orientation of the foliation (Fig. 2). This system was used to study the anisotropy of the fabric and, thus, its influence on physical rock properties.

2.2. Analyses

The texture of marbles was studied using an Olympus BX-60 polarized optical microscope (OM) coupled with digital microphotography (Olympus DP-10). Two thin sections were prepared in two orthogonal directions following the *XY*- and *YZ*-planes (Fig. 2a). Two more thin sections with the same orientation were filled with fluorochrome resin and then analyzed to identify the presence, aspect and distribution of fractures inside marbles.

To understand the spatial and geometrical configuration of all the components of a rock in terms of fabric and microstructure, we followed the methodology proposed by Passchier and Trouw (1996) which considers these parameters: grain size distribution, grain aspect ratio, preferred grain orientation, grain boundary morphology,

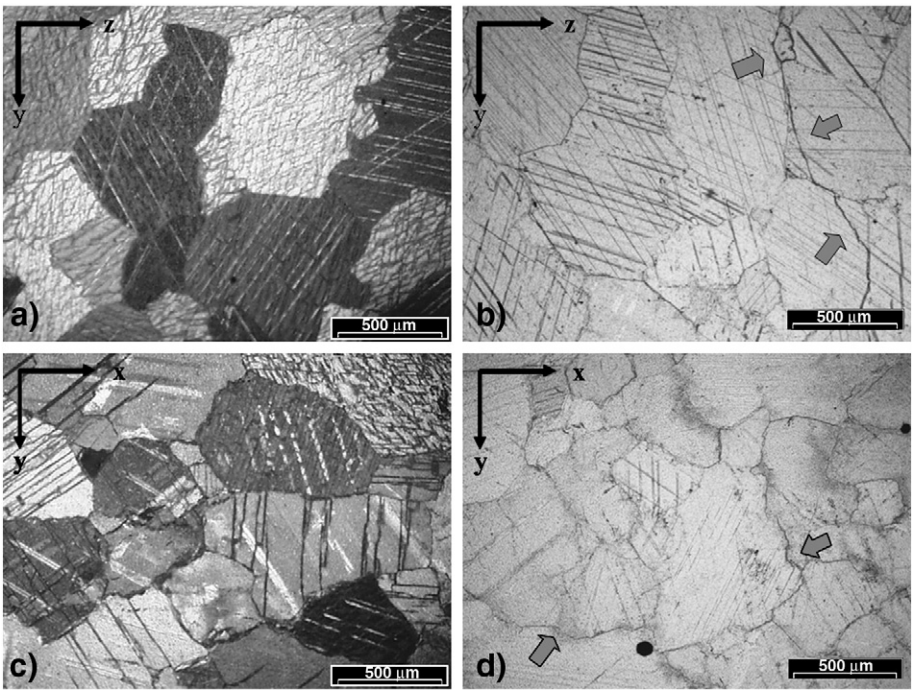

Fig. 4. Optical microphotographs of WM marble. a and b images show sections taken from the plane perpendicular to the foliation, while c and d images correspond to planes containing the foliation. Arrows indicate the development of both interparticle and intraparticle cracks along the *ZY* plane (image b), but only interparticle cracks along the *XY* plane (image d).

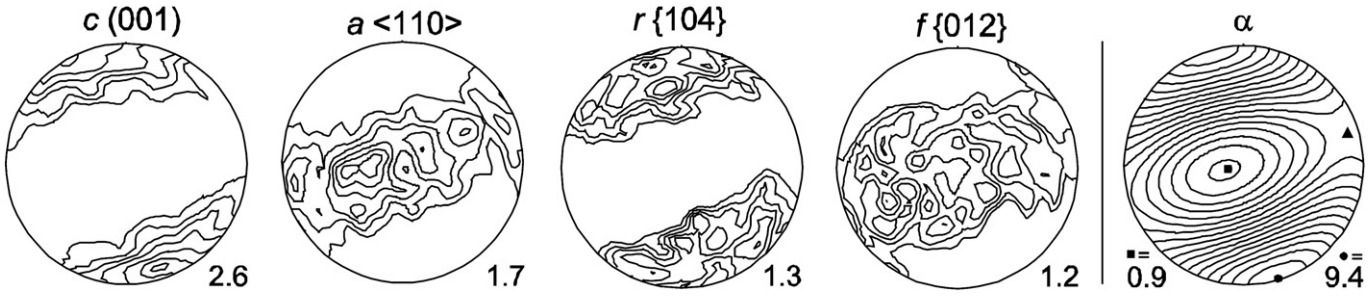

Fig. 5. Pole figures of calcite recalculated from the Orientation Distribution Function on the basis of X-ray diffraction measurements (equal area projection, lower hemisphere, maxima of multiples of random distribution (m.r.d.) are given, lowest contour line equals 1.0 m.r.d.). The plot on the right shows the distribution of the thermal dilatation coefficient α as calculated from the quantitative texture analysis (equal area projection, lower hemisphere, α_{min} and α_{max} [10^{-6}1/°C] are given).

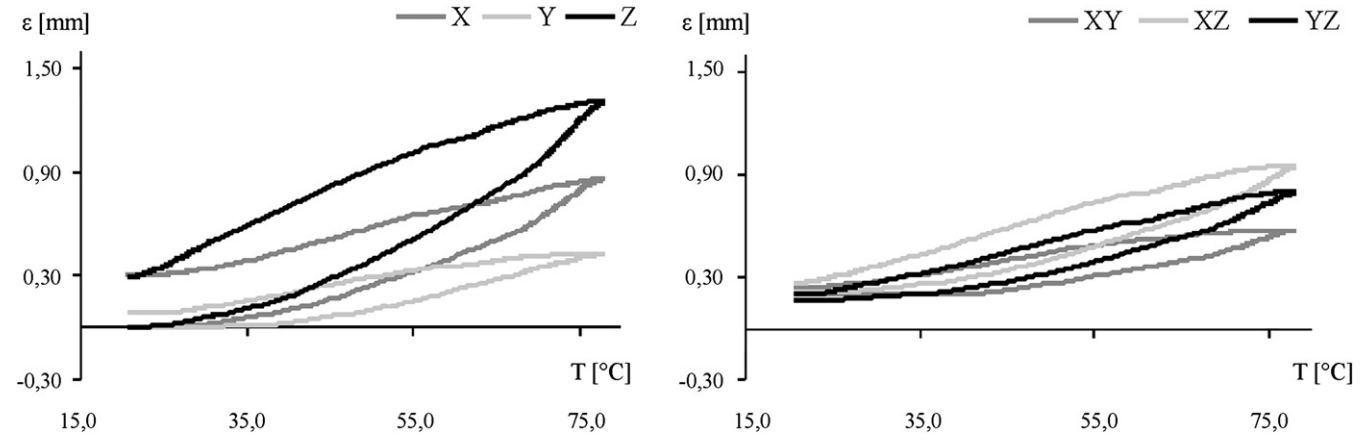

Fig. 6. Maximum expansion and residual strain of WM marble after the first and second thermal test cycle. In a) the three orthogonal axes *X*, *Y* and *Z* are represented, while in b) intermediate directions are shown.

grain boundary geometry, the size and orientation of microcracks and preferred lattice orientation.

Preferred crystallographic orientations were measured using a PANalytical X'pert System X-ray diffractometer (Leiss and Ullemeyer, 2006). A polycapillary on the primary beam side provided an optically parallel beam with a diameter of at least 7 mm. To further increase the number of grains measured, pole figures were measured at 13 different points on a sample of 70×70×10 mm. For the pole figure measurements, a 5°×5° (tilt/rotation angle) grid was applied. (006), <110>, {104}, {012}, {113} and {202}-pole figures were measured. The defocusing effect was corrected by polynomial functions derived from calcite powder measurements (Ullemeyer et al., 1998). Despite these corrections, data could only be used up to a tilt angle of 75° due to the increasing error of correction with increasing tilt angle. The 13 pole figures of each hkl were added. On the basis of the resulting experimental pole figures, an Orientation Distribution Function (ODF) was calculated by applying the iterative series-expansion method (Wenk et al., 1987; Dahms and Bunge, 1989). From the ODF complete pole figures were calculated. The bulk rock anisotropy of the thermal dilatation coefficient was calculated by applying the VOIGT averaging method (e.g. Bunge 1985) and is represented in an equal area projection.

Real and apparent density and open porosity were measured by forced water absorption according to the UNE-EN 1936 (2007) standard.

Of the various techniques for determining physical properties, ultrasound procedures are particularly useful because of their non-destructive nature. The measurements were performed with a Panametrics HV Pulser/Receiver 5058PR coupled with a Tektronix TDS 3012B oscilloscope. The propagation velocity of compressional (Vp) pulses was measured in accordance with the ASTM D 2845 (2005) standard on dry and wet test samples using polarized Panametric transducers of 1 GHz. These data were used to obtain information on the degree of compactness of the marbles (a decrease in the velocity showing the development of fissures).

The modifications in the distribution of the pore access size as well the pore/fissure volume of marbles before and after thermal stress test was determined using a Micromeritics Autopore III 9410 porosimeter with a maximum injection pressure of 414 MPa. Specimens of about 1 cm^3 were dried for 48 h at 50 °C and then analyzed. Two MIP measurements per sample were made.

6 drilled cores (15 mm diameter×50 mm length), orientated according to the pre-established axes, were cut and analyzed: 3 cores maintain the reference-coordinate directions (*X*-, *Y*- and *Z*-) while the other 3 cores show intermediate directions (*XY*-, *XZ*- and *YZ*-) (Fig. 3). We measured the ultrasound wave velocity under controlled heat and humidity conditions (~25 ºC and relative humidity of ~50%). A viscoelastic couplant was used to ensure good coupling between transducers and marble samples. The transmission

Table 1
Representation of the maximum WM elongation and linear thermal expansion coefficients (α) along each axis when temperature increases in the range from 25 to 90 °C.

BM axes	Maximum elongation (ε, mm/m)	Thermal expansion coefficient (α, 10^{-6}/K)	Residual strain (mm)
X	0.86	16.673	0.32
Y	0.43	9.522	0.09
Z	1.31	23.976	0.29
XY	0.53	11.892	0.20
XZ	0.87	17.609	0.22
YZ	0.77	14.982	0.17

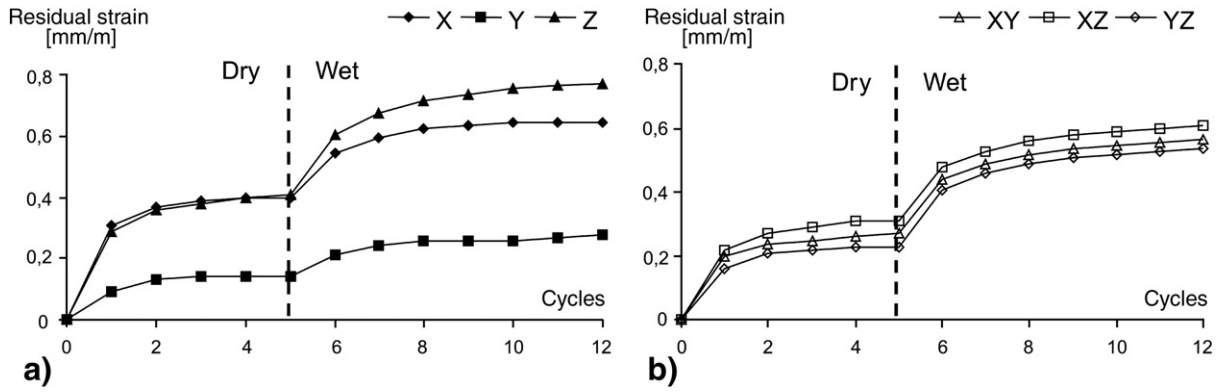

Fig. 7. Residual strain increase of WM marble over 5 dry cycles and then 7 wet cycles in three orthogonal axes *X*, *Y* and *Z* (a) and along intermediate directions (b).

method was used and three measurements were taken for each direction under consideration.

The degree of anisotropy of the WM marble was evaluated by performing a thermal expansion test with respect to certain specific orientations (*X*, *Y*, *Z*, *XY*, *XZ* and *YZ*). The cores used for the ultrasound and water absorption tests, once indexed according to the coordinate system, were used again in this test.

The test carried out in this work is the test proposed by Koch and Siegesmund (2004) in which a chamber allows the simultaneous analysis of six samples. 12 cycles were carried out: 5 in dry conditions and 7 under wet conditions.

In order to simulate temperature changes similar to those observed in buildings, each cycle maintains the temperature interval of 20 ºC to 90 ºC and back down to 20 °C again over 15 h in dry conditions while 17 h in wet conditions. The heating rate was 1 °C per minute to ensure the thermal equilibration of specimens.

The thermal expansion coefficient (α, in $10^{-6}K^{-1}$) expresses the relative change in length (or volume) of the stone according to changes in temperature. In most calcitic marbles, α is non-linear and depends on the temperature interval used (Siegesmund et al., 2008). It is calculated according to the following equation:

$$\alpha = \Delta l / (l \times \Delta T) \quad (1)$$

where:

Δl is the change in length of the sample (mm)
l is the length of sample (mm)
ΔT is the temperature interval (K).

Thermal expansion (ε_{rs} in mm/m) represents the relationship between the change in length of the sample after cooling down to room temperature and the original sample length and is defined as:

$$\varepsilon_{rs} = \Delta l_{rt} / l_r \quad (2)$$

where:

Δl_{rt} is the change in length of the sample after cooling down to room temperature (mm)
l_r is the original length of the sample for a given temperature range (mm).

The residual strain (r in mm) generated by the thermal expansion is the irreversible damage that takes place in a sample once it returns to its initial (environmental) temperature. This parameter is related to anisotropic thermal expansion.

Generally, samples that undergo this test show four types of behaviour which are characterized by: a) isotropic thermal expansion without residual strain; b) isotropic thermal expansion with residual strain; c) anisotropic thermal expansion without residual strain and d) anisotropic thermal expansion with residual strain (Weiss et al., 2003).

3. Results and discussion

3.1. Mineralogy and texture

Under optical microscopy, WM shows a typical poligonal granoblastic texture with equidimensional shapes and grains of very varied sizes (between 0.1 and 3 mm). This texture clearly indicates a static recrystallization, in which the grain boundaries become straighter and grains increase in size becoming hexagonal in shape. These two processes finally produce a reduction of grain boundary area and, therefore, a reduction of the total energy of the crystalline aggregate (Passchier and Trouw, 1996).

When we analyzed the sections prepared with fluorochrome resin, we observed that the lines that mark the grain boundaries showed different degrees of union depending on the orientation of the marble

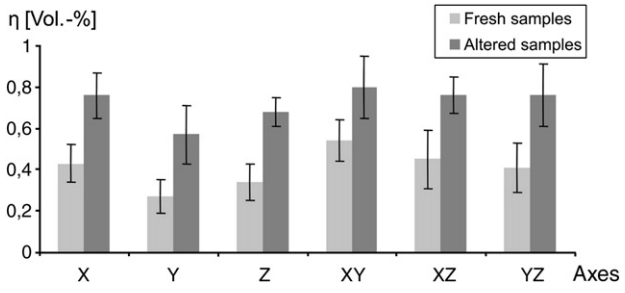

Fig. 8. WM pore volume change (η in %) before and after heat treatment.

Table 2
Porosimetric parameters of White Macael marble before and after thermal treatment.

	Fresh samples	Altered samples
Total Pore Area (m^2/g)	0.185 ± 0.55	1.342 ± 0.76
Apparent density (g/cm^3)	2.676 ± 0.05	2.548 ± 0.06
Real density (g/cm^3)	2.724 ± 0.09	2.729 ± 0.06
Porosity (%)	1.780 ± 0.90	6.628 ± 1.25

Average values are presented for fresh and altered marble.

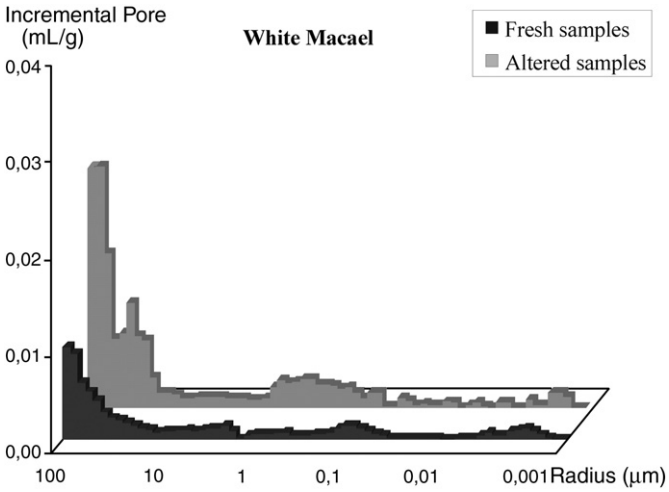

Fig. 9. Pore size distribution curves for White Macael marble measured in fresh and altered samples.

(Fig. 4b and d). In fact, on the surface defined by *ZY* axes the grain boundaries were straight, while on the *XY* surface, they present a degree of suturing, suggesting a sintering mechanism among crystals. Furthermore, we must also consider the morphology of pre-existing fissures in marble because these are different on each plane; on the *ZY* plane they are intra- and interparticles and follow a rectilinear morphology, while along the *XY* plane they are only interparticles, and are sinuous in shape.

Finally, small amounts of quartz, phyllosilicates (i.e., muscovite), iron oxides and opaque minerals, probably pyrite, were also detected. These opaque minerals enable us to detect the foliation planes even with the naked eye.

The results of the texture analyses are represented by pole diagrams in Fig. 5. According to the Leiss and Weiss (2000)) classification, the texture of WM marble can be defined as *c*-axis fibre-type because the *c*-axis maxima are clearly developed and the *a*-axis maxima are quite regularly distributed on a great circle. The *c*-axis maximum is only of moderate intensity and pseudo-normal oriented to the regional foliation.

3.2. Thermal expansion

The results of the thermal expansion test under dry conditions (Fig. 6a) show that the greatest elongation occurs along the *Z*-axis (1.31 mm/m) and the lowest is recorded by the *Y*-axis (0.43 mm/m) which is normal to the *Z*-axis and parallel to the foliation plane. *XY*, *YZ* and *XZ* directions show intermediate values. However, only the relation between the orthogonal (*X*-, *Y*- and *Z*-axes) values denotes the strong anisotropy of this marble ($A\alpha = \alpha_{min}/\alpha_{max} = 0.40\%$ and $A\varepsilon = \varepsilon_{min}/\varepsilon_{max} = 0.33\%$).

Table 3
Schematic representation of Vp values in fresh and deteriorated (*) samples.

BM Axes	Vp (m/s)	Vp* (m/s)	ΔVp1 − Vp1*	η (%)	η (%)*	Δη (%)
X	5885	2647	3440	0.43	0.76	0.33
Y	5756	3625	2423	0.27	0.57	0.3
Z	5058	2794	2564	0.34	0.68	0.35
XY	5421	3726	1695	0.54	0.8	0.25
XZ	5549	3174	2375	0.45	0.76	0.31
YZ	5422	3009	2413	0.41	0.76	0.35

Porosity (η) and differential values (ΔVp and $\Delta\eta$) are also shown.

There seems to be a correlation between residual strain values and the anisotropy of thermal expansion. Along the direction of α-max, residual tension (0.29 mm) is three times as high as that obtained along α-min (0.09 mm). The residual strain shows that WM deforms irreversibly in the *z*-axis direction, especially after the first heating cycle.

Modal composition is known to have an influence on the thermal properties of marble. According to Kleber (1959), the thermal expansion coefficient (α) of calcite is $26\times10^{-6}K^{-1}$ in the direction parallel to the *c*-axis and $-6\times10^{-6}K^{-1}$ in the parallel to the *a*-axis. In the case of WM marble, the maximum and minimum α values correspond to the *Z*- and *Y*-axes respectively, which indicates that there is a direct link between the preferential orientation of the axes and the crystalline structure of marble (Table 1).

Nevertheless, according to Siegesmund et al. (1997, 2000), the residual strain produced for each direction is also influenced by the fabric of the rock and by the existence of microcracks prior to the test.

The behaviour of the marble under the thermohydric expansion test was similar to that observed under dry conditions. The values for residual strain obtained in the six directions selected in WM marble showed a continued growth during the test cycles. Although the residual strain values remained constant between the third and fifth cycle, in the following cycles and under wet conditions, all samples were characterized by a further, progressive expansion (Fig. 7).

The low porosity of fresh WM marble ($\bar{\eta} = 0.41\%$) indicates that some, albeit few microcracks existed prior to the test. This is a useful value for evaluating the durability of marble when subjected to thermal changes. In fact, in all the samples we tested we observed a slight increase in porosity ($\bar{\eta} = 0.72\%$) after the thermal expansion test (Fig. 8). Although this increase may be insignificant, it should not be ignored since an increase in fissure porosity can influence the durability of the material. According to the (Köhler, 1991) classification, after the thermal expansion test, the WM marble moves from fresh to increasingly porous material.

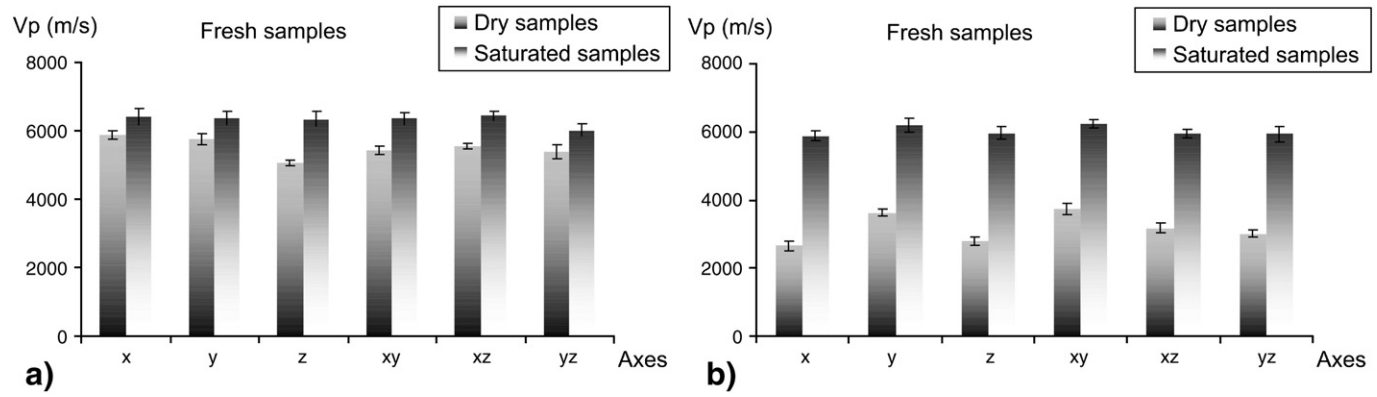

Fig. 10. Ultrasound wave velocities measured in dry and saturated samples. Image a) shows fresh samples while b) are deteriorated samples.

The increase in porosity was clearly evidenced after MIP tests. In fact, changes in the rank of pore size and in the total porosity were detected after thermal treatment (Table 2). The augment in the volume of larger pores/fissures (Fig. 9) is important because they will be new ways to other decay agents (water, salts, etc.).

If we compare the data for forced water absorption with those for ultrasounds we can see that both tests indicate an increase in porosity and, therefore, incipient decay. If we analyze the ultrasound data in greater detail, the values for quarry samples are lower than that for a single calcite crystal (Fig. 10) suggesting that microcracks may exist. In addition, if we start from the values obtained in the three orthogonal directions (*X*-, *Y*- and *Z*-axes), WM marble shows a high textural anisotropy ($\Delta M = 13\%$), which is also due to the anisotropy introduced by calcite single crystals and the pre-existing microcracks (Siegesmund et al., 1999).

Finally, the strong decrease of Vp values in altered samples (Table 3) confirms the increase in porosity.

4. Discussions and conclusions

After determining the texture and the crystallographic orientation of calcite grains, we observed that calcite crystals showed *c*-axis orientation pseudo-parallel to the *Z*-axis. This suggests that these axes are situated perpendicular to the foliation plane while the *a*-axis is parallel to the foliation plane.

The petrographic study revealed that most of the calcite crystals are granoblastic with equidimensional shapes (i.e. pseudo-hexagonal) and various different sizes. We can also see that the union between the grains varies depending on the orientation of the marble. The surface parallel to the foliation plane (*XY*) shows a winding grain boundary and we can also see that some of these boundaries have strong suture lines. In the surface perpendicular to the *ZY* plane, the grain boundary is almost a straight line, with the presence of triple-points, weak boundary lines and intra- and interparticle microcracks. As suggested by Siegesmund et al. (1999), the degree and geometry of deformation are connected by different shapes, fabrics and textures.

On the basis of the research carried out to assess the damage that temperature changes produce in marble, it is evident that two of the most important factors affecting behaviour are the shape of the grains, and the grain boundaries. In White Macael marble we have observed that both the pseudo-hexagonal shape of the grain and the straight grain boundaries mean that it is less resistant to thermal change than crystal samples with irregular shapes and curved or complex grain boundaries. It was also observed that weak grain boundaries facilitate dilation to a large extent and this leads to the propagation of cracks and the appearance of gaps (Malaga et al., 2008).

Moreover, the volume of pores calculated by water absorption and confirmed by ultrasound data indicates the pre-existence of microcracks within the marble, which in this case were also identified by optical microscopy for both the *XY* and *YZ* planes.

We can conclude that WM marble is not an ideal material in terms of durability criteria, as the anisotropy of the marble (due to the anisotropy of the calcite), the texture (grain size, grain boundaries and the preferred crystallographic orientation) and the pre-existence of microcracks are all important negative factors in marble behaviour during heat treatment–water cycles.

Thermal expansion results show the high dilation coefficient measured in White Macael marble in two of its three orthogonal directions (*X* and *Z* axes) and also the increase in residual strain produced during heating cycles in the presence of water. These results must be taken into account when trying to evaluate marble durability since, although Rodríguez-Gordillo and Sáez-Pérez (2006) observed a decrease of Vp values after the first 50 cycles, this velocity remained constant throughout the other cycles. However, the test with moisture change shows that the increase in residual strain with the increase of cycles under wet conditions leads to a higher granular disintegration and, therefore, a sharper reduction in velocity during the following cycles.

We can therefore conclude that the heat treatment causes significant decay in White Macael marble, and that this decay can be measured by means of the techniques used in the present research. Data obtained from the ultrasound test in different directions and the increase in porosity after the thermal test clearly indicate the loss of cohesion between the grains. From this moment on White Macael marble must be treated as a porous material.

Given that the intrinsic properties of this marble do not favour its durability in the above-mentioned weathering conditions, it is probable that its initial state of deterioration will be enhanced by other decay agents (e.g. soluble salts).

The results provided in this research can be used as a guide in the restoration of other artworks or monuments manufactured with White Macael marble.

Acknowledgements

This research has been supported by the Research Projects FQM 1635 and HA 2007-0012 and by the Research Group of the Junta de Andalucía RNM 179. We thank Nigel Walkington for the translation of the manuscript.

References

Åkesson, U., Lindqvist, J.E., Schouenborg, B., Grelk, B., 2006. Relationship between microstructure and bowing properties of calcite marble claddings. Bull. Eng. Geol. Environ. 65, 73–79.

ASTM D 2845-05, 2005. Standard method for laboratory determination of pulse velocities and ultrasonic elastic constants of rock. Pennsylvania: ASTM International Standards Worldwide, p1–7.

Balanyá, J.C., García-Dueñas, V., 1986. Grandes fallas de contracción y de extensión implicadas en el contacto entre los dominios de Alborán y Sudibérico en el Arco de Gibraltar. Geogaceta 1, 19–21.

Battaglia, S., Franzini, M., Mango, F., 1993. High sensitivity apparatus for measuring linear thermal expansion: preliminary results on the response of marbles. Il Nuovo Cimiento 16, 453–461.

Bello, M.A., Martín, L., Martín, A., 1992. Decay and treatment of macael white marble. Stud. Conserv. 37, 193–200.

Bland, W., Rolls, D., 1998. Weathering. Arnold, London. 271 pp.

Bortz, S.A., Erlin, B., Monk, C.B., 1988. Some field problems with thin veneer building stones. New Stone Technology, Design and Construction for Exterior Wall Systems. American Society for Testing and Materials, Philadelphia, pp. 11–31.

Bunge, H.J., 1985. Physical properties of polycrystals. In: Wenk, H.-R. (Ed.), Preferred Orientation in Deformed Metals and Rocks: An Introduction to Modern Texture Analysis. Academic Press, pp. 507–525.

Cantisani, E., Pecchioni, E., Fratini, F., Garzonio, C.A., Malesani, P., Molli, G., 2009. Thermal stress in the Apuan marbles: relationship between microstucture and petrophysical characteristics. International Journal of Rock Mechanics and Mining Sciences 46, 128–137.

Dahms, M., Bunge, H.-J., 1989. The iterative series-expansion method for quantitative texture analysis. I. General outline. J. Appl. Cryst. 22, 439–447.

Galán, E., Zezza, F., 1990. Diagnóstico del estado de conservación del Patio de los Leones de la Alhambra de Granada. Informe para el Patronato de la Alhambra y Generalife, Granada.

Kessler, D.W., 1919. Physical and chemical test of the commercial marbles of the United States. Technologic Papers of the Bureau of Standards, 123. Government Printing Office, Washington D.C.

Kleber, W., 1959. Einführung in die Kristallographie. VEB Verlag Technik, Berlin, Germany.

Koch, A., Siegesmund, S., 2002. Bowing of marble panels: on-site damage analysis from the Oeconomicum Building at Göttingen (Germany). In: Siegesmund, S., Weiss, T., Vollbrecht, A. (Eds.), Natural Stone, Weathering Phenomena, Conservation Strategies and Case Studies. Geological Society, London, pp. 299–314.

Koch, A., Siegesmund, S., 2004. The combined effect of moisture and temperature on the anomalous expansion behaviour of marble. Env. Geol. 46, 350–363.

Köhler, W., 1991. Untersuchungen zu Verwitterungsvorgängen an Carrara-Marmor in Potsdam-Sanssouci. Berichte zu Forschung und Praxis der Denkmalpflege in Deutschland: Steinschäden - Steinkonservierung, 2, pp. 50–53.

Leiss, B., Ullemeyer, K., 2006. Neue Perspektiven der Texturanalytik von Gesteinen mit konventioneller Röntgenbeugung. In: Philipp, S.L., Leiss, B., Vollbrecht, A., Tanner, D., Gudmundsson, A. (Eds.), 11. Symposium,Tektonik, Struktur- und Kristallingeologie'. Extended Abstracts. Universitätsverlag Göttingen, pp. 128–130.

Leiss, B., Weiss, T., 2000. Fabric anisotropy and its influence on physical weathering of different types of Carrara Marbles. J Struct Geol. 22, 1737–1745.

López Sánchez-Vizcaíno, V., Connolly, J.A.D., Gómez-Pugnaire, M.T., 1997. Metamorphism and phase relations in carbonate rocks from the Nevado-Filabride Complex (Cordilleras Béticas, Spain): application of the Ttn + Rt + Cal + Qtz + Gr buffer. Contrib. Mineral. Petrol. 126, 292–302.

Malaga, K., Schouenborg, B., Grelk, B., 2008. Bowing and expansion of natural stone panels: marble and limestone testing and assessment. Materiales de Construcción 58, 97–112.

Passchier, C.W., Trouw, R.A.J., 1996. Microtectonics. Springer, Berlin Heidelberg New York.

Rodríguez-Gordillo, J., Sáez-Pérez, M.P., 2006. Effects of the thermal changes on Macael marble: experimental study. Constr. Build. Mater. 20, 355–365.

Royer-Carfagni, G., 2000. Some considerations on the warping of marble facades: the example of Alvar Aaltos Finland Hall in Helsinki. Constr. Build. Mater. 13, 449–457.

Sáez-Pérez, M.P., Rodríguez-Gordillo, J., 2009. Structural and compositional anisotropy in Macael marble (Spain) by ultrasonic, XRD and optical microscopy methods. Construction and Building Materials 23, 2121–2126.

Siegesmund, S., Vollbrecht, A., Ullemeyer, K., Weiss, T., Sobott, R., 1997. Anwendung der geologischen Gefügekunde zur Charakterisierunfg natürlicher Weksteine - Fallbeispiel: Kauffunger Marmor. International Journal for Restoration of Buildings and Monuments 3, 269–292.

Siegesmund, S., Weiss, T., Vollbrecht, A., Ullemeyer, K., 1999. Marble as natural building stone: rock fabrics, physical and mechanical properties. Thermenheft Marmorkonservierung. Z dt geol Ges 150 (2), 237–506.

Siegesmund, S., Ullermeyer, K., Weiss, T., Tschegg, E.K., 2000. Physical weathering of marbles caused by anisotropic thermal expansion. Int J Earth Sci 89, 170–182.

Siegesmund, S., Ruedrich, J., Koch, A., 2008. Marble bowing: comparative studies of three different public building facades. Environmental Geology, In press.

Strohmeyer, D., 2004. Naturwerksteine: Gefuege und gesteins-technische Eigenschaften. University of Goettingen, Doctoral thesis.

Thomasen, S.E., Ewart, C.S., 1984. Durability of the thin-set marble. Third International Conference on Durability of Building Materials and Components, pp. 313–323.

Ullemeyer, K., Spalthoff, P., Heinitz, J., Isakov, N.N., Nikitin, A.N., Weber, K., 1998. The SKAT texture diffractometer at the pulsed reactor IBR-2 at Dubna: experimental layout and first measurements. Nuclear Instruments and Methods in Physics Research Section A: Accelerators, Spectrometers, Detectors and Associated Equipment 412, 80–88.

UNE-EN 1936, 2007. Métodos de ensayo para piedra natural. Determinación de la densidad real y aparente y de la porosidad abierta y total. AENOR, Madrid.

Weiss, T., Siegesmund, S., Rasolofosaon, P., 2000. The relationship between deterioration, fabric, velocity and porosity constraint. 9th International congress on Deterioration and Conservation of Stone, Venice, pp. 19–24.

Weiss, T., Siegesmund, S., Fuller, ER., 2002. Thermal stresses and microcracking in calcite and dolomite marbles via finite element modelling. In: Siegesmund, S., Weiss, T., Vollbrecht, A. (Eds.), Natural Stone, Weathering Phenomena, Conservation Strategies and Case Studies. Geological Society, London, pp. 65–80.

Weiss, T., Siegesmund, S., Fuller, E., 2003. Thermal degradation of marbles: indications from finite element modelling. Building Environment 38, 1251–1260.

Wenk, H.R., Takeshita, T., Bechler, E., Erskine, B.G., Matthhies, S., 1987. Pure shear and simple shear on calcite textures. Comparison of experimental, theoretical and natural data. Journal of Structural Geology 9, 371–745.

Widhalm, C., Tschegg, E., Eppensteiner, W., 1996. Anisotropic thermal expansion causes deformation of marble cladding. J. Perform. Constr. Facil. 10, 5–10.

Widhalm, C., Tschegg, E., Eppensteiner, W., 1997. Acoustic emission and anisotropic expansion when heating marble. J. Perform. Constr. Facil. 11, 35–40.

Zeisig, A., Siegesmund, S., Weiss, T., 2002. Thermal expansion and its control on the durability of marbles. In: Siegesmund, S., Weiss, T., Vollbrecht, A. (Eds.), Natural Stone, Weathering Phenomena, Conservation Strategies and Case Studies. Geological Society, London, pp. 65–80.

Zezza, U., Sebastián Pardo, E.M., 1992. El mármol de Macael en los monumentos históricos de Granada (España). Proceedings I International Congress. Rehabilitación del Patrimonio Arquitectónico 1, 153–162.